Mechanics of Advanced Composite Structures 6 (2019) 65–74

Semnan University

Mechanics of Advanced Composite Structures

journal homepage: http://MACS.journals.semnan.ac.ir

Non-Linear Analysis of Functionally Graded Sector Plates with Simply Supported Radial Edges Under Transverse Loading

F. Fallah*, M.H. Karimi

Department of Mechanical Engineering, Sharif University of Technology, P.O. Box 11365-9567, Azadi Avenue, Tehran, Iran

PAPER INFO

Paper history:
Received 2018-10-14
Received in revised form 2019-01-15
Accepted 2019-04-26

Keywords:
Functionally graded Materials
First-order shear deformation plate theory
Sectorial plate
Nonlinear analysis
Perturbation technique

ABSTRACT

In this study, nonlinear bending of functionally graded (FG) circular sector plates with simply supported radial edges subjected to transverse mechanical loading has been investigated. Based on the first-order shear deformation plate theory with von Karman strain-displacement relations, the nonlinear equilibrium equations of sector plates are obtained. Introducing a stress function and a potential function, the governing equations which are five non-linear coupled equations with total order of ten are reformulated into three uncoupled ones including one linear edge-zone equation and two nonlinear interior equations with total order of ten. The uncoupling makes it possible to present analytical solution for nonlinear behavior of FG sector plates with simply-supported radial edges via perturbation technique and Fourier series method. The material properties are graded through the plate thickness according to a power-law distribution of the volume fraction of the constituents. The results are verified by comparison with the existing ones in the literature. The effects of non-linearity, material constant and boundary conditions on bending of an FG sector plate are studied. It is shown that in bending analysis of functionally graded sector plates, linear theory is solely applicable for $w/h < 0.2$ and is inadequate for analysis of fully simply supported FG sector plates even in the small deflection range.

1. Introduction

Functionally graded materials (FGMs) were first introduced in 1984 by material scientists in Japan [1]. These materials are heterogeneous and are made of at least two constituents. Furthermore, their properties vary continuously by gradually changing the volume fraction of the constituent materials along certain directions. They have found many applications in different fields due to their smooth variation in properties including spacecraft heat shields, heat exchanger tubes, biomedical implants, and flywheels [2].

Sector plates have a wide range of engineering applications such as basic structural elements, curved bridge decks, building floor slabs, and steam turbine diaphragms [3]. Therefore, understanding the mechanical behavior of sector plates is necessary. Based on the first-order shear deformation plate theory (FSDT), Ambartsumyan [4] presented an exact analytical solution for bending analysis of isotropic homogenous sector plates with two radial edges simply supported under uniform loading. Cheung and Chen [5] employed the finite strip method for static and dynamic analyses of thin and thick sectorial plates. Lie and Liew [6] adopted the differential quadrature method for a static analysis of annular sectorial plates based on FSDT. Lim and Wang [7] developed relationships between the Mindlin plate results and the corresponding Kirchhoff plate solutions for bending of annular sectorial plates with simply supported radial edges. Based on the FSDT, Jomehzadeh and Saidi [8] presented an exact

* Corresponding author. Tel.: +98-21-66165516; Fax: +98-21-66000021
E-mail address: fallah@sharif.ir

DOI: 10.22075/MACS.2019.16171.1167

analytical approach for bending analysis of FG annular sector plates. Developing a reformulation of the governing equations within FSDT, Fallah and Nosier [9] presented an analytical closed-form solution for bending of FG circular sector plates with simple supports at their radial edges, and subjected to thermo-mechanical loadings. Based on FSDT, Mousavi and Tahani [10] analyzed bending behavior of radially functionally graded (RFG) sector plates using multi-term extended Kantorovich method. Based on classical plate theory (CLPT) of thin plates, Fereidoon and Mohyeddin [11] proposed a semi-analytical solution for bending behavior of thin functionally graded sector plates with various types of supports under uniform and non-uniform loadings. Aghdam and Shahmansouri [12] studied the bending of moderately thick clamped FG sector plates using FSDT and extended Kantorovich method (EKM). Fallah and Khakbaz [13] studied the bending behavior of functionally graded annular sector plates with arbitrary boundary conditions subjected to both uniform and non-uniform loadings in terms of FSDT and single-term EKM. They employed EKM in two approaches. In the first one, they applied EKM to the displacement field and the functional form of the problem and in the second one, they applied EKM to the weighted integral form of the governing equations. They showed that while both approaches give accurate results for clamped and simply-supported boundary conditions, but just the first approach is acceptable for analysis of plates with free edges. Turvey and Salehi [14] used a finite-difference discretization and dynamic relaxation algorithm to solve the elastic large deflection equations of isotropic sector plates. Alinaghizadeh and Kadkhodayan [15] carried out nonlinear bending analysis of radially FG circular sector plates on elastic foundation using FSDT and non-linear von Kármán assumptions. They employed generalized differential quadrature method and Newton–Raphson iterative scheme to solve the nonlinear equations. Golmakan and Kadkhodayan [16] used dynamic relaxation numerical method and finite difference discretization technique to analyze large deflection behavior of stiffened annular FG sector plates under mechanical and thermo-mechanical loadings. From the literature review it is evident that most studies on bending behavior of FG sector plates are limited to linear analyses [8-13], while nonlinear analyses are few and are based on numerical methods [15, 16]. In addition, to the best of authors' knowledge, there is no effort reported on large deflection response of FG sector plates whose effective properties vary through the thickness direction.

In this study, based on FSDT and von Karman type of nonlinearity, nonlinear bending of FG circular sector plates with simple supports at their radial edges and subjected to transverse mechanical load is analytically studied. The material properties are assumed to be graded through the plate thickness according to a power-law distribution of the volume fraction of the constituents. Reformulation of non-linear coupled equilibrium equations into three uncoupled ones makes it possible to present analytical solution employing perturbation technique and Fourier series expansions. The results are verified by comparison with the existing ones in the literature. Effects of nonlinearity and material constant on bending behaviour of FG sector plates with simply supported and clamped circumferential edges are investigated. The results presented can be used as a benchmark in future studies.

2. Theoretical formulation

A functionally graded circular sector plate with outer radii of b, vertex angle θ_0, and thickness h under transverse loading is considered. The geometry of the sector plate, loading and the coordinate system are shown in Fig. 1. The sector plate has simply supports at radial edges and arbitrary boundary conditions along the circumferential edge.

Here, functionally graded material is modeled as a non-homogeneous isotropic elastic material and is assumed to be composed of ceramic (upper surface) and metal (lower surface) whose Young's modulus vary continuously through the thickness of the plate according to a power-law relation in (1) [9]:

$$E(z) = (E_m - E_c)\left(\frac{h-2z}{2h}\right)^n + E_c \qquad (1)$$

where the subscripts c and m refer to ceramic and metal, respectively and n is the power-law index that takes values greater than or equal to zero. The Poisson ratio v is assumed to be constant through the plate thickness.

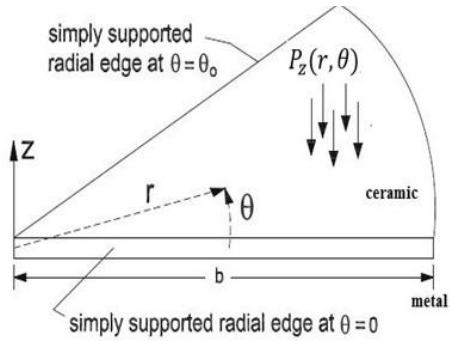

Fig. 1. Geometry of FG solid circular sector plate under a uniform pressure and the coordinate system

2.1. Equilibrium equations

The displacement field of the plate in polar coordinate within the first-order shear deformation plate theory is assumed as follows [18],

$$U(r,\theta,z) = u(r,\theta) + z\Psi_r(r,\theta)$$
$$V(r,\theta,z) = v(r,\theta) + z\Psi_\theta(r,\theta) \quad (2)$$
$$W(r,\theta,z) = w(r,\theta)$$

where u, v, and w represent the displacement components of a point on the middle plane of the plate along r, θ , and z directions, respectively. Also, Ψ_r and Ψ_θ are the rotations of a transverse normal about the θ- and r-axes, respectively. Substituting Eq. (2) into the von Karman nonlinear kinematic relations [17] the nonzero strain components are found as follows:

$$\begin{aligned}
&\varepsilon_r = \varepsilon_r^0 + zk_r\\
&\varepsilon_\theta = \varepsilon_\theta^0 + zk_\theta\\
&\gamma_{\theta z} = k_{\theta z}\\
&\gamma_{rz} = k_{rz}\\
&\gamma_{r\theta} = \gamma_{r\theta}^0 + zk_{r\theta}
\end{aligned} \quad (3)$$

where

$$\begin{aligned}
&\varepsilon_r^0 = u_{,r} + \frac{1}{2}\left(w_{,r}\right)^2\\
&\varepsilon_\theta^0 = \frac{1}{r}\left(u + v_{,\theta}\right) + \frac{1}{2}\frac{1}{r^2}\left(w_{,\theta}\right)^2\\
&\gamma_{r\theta}^0 = \frac{1}{r}\left(u_{,\theta} - v\right) + v_{,r} + \frac{1}{r}w_{,r}w_{,\theta}\\
&k_r = \psi_{r,r}\\
&k_\theta = \frac{1}{r}\left(\psi_r + \psi_{\theta,\theta}\right)\\
&k_{r\theta} = \frac{1}{r}\left(\psi_{r,\theta} - \psi_\theta\right) + \psi_{\theta,r}\\
&k_{\theta z} = \frac{1}{r}w_{,\theta} + \psi_\theta\\
&k_{rz} = \psi_r + w_{,r}
\end{aligned} \quad (4)$$

in which a comma followed by a coordinate variable designates partial derivative with respect to that variable. By employing the principle of minimum total potential energy [17] and using Eqs. (3) and (4), the equilibrium equations governing the behavior of an FG circular sector plate under transverse loading $\boldsymbol{P_z(r,\theta)}$ (see Fig.1) are obtained as follows:

$$\delta u;\quad N_{r,r} + \tfrac{1}{r}(N_r - N_\theta) + \tfrac{1}{r}N_{r\theta,\theta} = 0$$
$$\delta v;\quad N_{r\theta,r} + \tfrac{1}{r}N_{\theta,\theta} + \tfrac{2}{r}N_{r\theta} = 0 \quad (5a)$$
$$\delta\psi_r;\ M_{r,r} + \tfrac{1}{r}(M_r - M_\theta) + \tfrac{1}{r}M_{r\theta,\theta} - Q_r = 0 \quad (5b)$$
$$\delta\psi_\theta;\ M_{r\theta,r} + \tfrac{1}{r}M_{\theta,\theta} + \tfrac{2}{r}M_{r\theta} - Q_\theta = 0$$
$$\delta w;\quad rQ_{r,r} + Q_{\theta,\theta} + Q_r = rP_z(r,\theta) - rN_1 \quad (5c)$$

where N_1 is defined as:

$$N_1 = N_r w_{,rr} + N_\theta\left(\frac{1}{r}w_{,r} + \frac{1}{r^2}w_{,\theta\theta}\right) + 2N_{r\theta}\left(\frac{1}{r}w_{,\theta}\right)_{,r} \quad (6)$$

The stress and moment resultants in (5) are defined as follows:

$$(N_r, N_\theta, N_{r\theta}, Q_\theta, Q_r) = \int_{-\frac{h}{2}}^{\frac{h}{2}}(\sigma_r, \sigma_\theta, \sigma_{r\theta}, \sigma_{\theta z}, \sigma_{rz})\,dz$$
$$(M_r, M_\theta, M_{r\theta}) = \int_{-\frac{h}{2}}^{\frac{h}{2}}(\sigma_r, \sigma_\theta, \sigma_{r\theta})z\,dz \quad (7)$$

Considering the plane-stress state, the linear elastic constitutive equations are as follows [18]:

$$\begin{Bmatrix}\sigma_r\\ \sigma_\theta\\ \sigma_{r\theta}\end{Bmatrix} = \frac{E(z)}{(1-v^2)}\begin{bmatrix}1 & v & 0\\ v & 1 & 0\\ 0 & 0 & \frac{1-v}{2}\end{bmatrix}\begin{Bmatrix}\varepsilon_r\\ \varepsilon_\theta\\ \gamma_{r\theta}\end{Bmatrix} \quad (8)$$
$$\begin{Bmatrix}\sigma_{\theta z}\\ \sigma_{rz}\end{Bmatrix} = k^2\frac{E(z)}{2(1+v)}\begin{bmatrix}1 & 0\\ 0 & 1\end{bmatrix}\begin{Bmatrix}\gamma_{\theta z}\\ \gamma_{rz}\end{Bmatrix}$$

where K^2 is a shear correction factor. Upon substitution of Eqs. (3) into (8) and the ensuing results into (7), the stress and moment resultants are obtained

$$N_r = A_1\varepsilon_r^0 + (A_1 - 2A_2)\varepsilon_\theta^0 + B_1k_r + (B_1 - 2B_2)k_\theta$$
$$N_\theta = (A_1 - 2A_2)\varepsilon_r^0 + A_1\varepsilon_\theta^0 + (B_1 - 2B_2)k_r + B_1k_\theta$$
$$N_{r\theta} = A_2\gamma_{r\theta}^0 + B_2k_{r\theta} \quad (9a)$$
$$M_r = B_1\varepsilon_r^0 + (B_1 - 2B_2)\varepsilon_\theta^0 + D_1k_r + (D_1 - 2D_2)k_\theta$$
$$M_r = (B_1 - 2B_2)\varepsilon_r^0 + B_1\varepsilon_\theta^0 + (D_1 - 2D_2)k_r + D_1k_\theta$$
$$M_{r\theta} = B_2\gamma_{r\theta}^0 + D_2k_{r\theta} \quad (9b)$$
$$Q_\theta = K^2A_2k_{\theta z},\ Q_r = K^2A_2k_{rz} \quad (9c)$$

where the stiffness coefficients are defined as:

$$(A_1, B_1, D_1) = \int_{-h/2}^{h/2}\frac{E(z)}{(1-v^2)}(1, z, z^2)dz$$
$$(A_2, B_2, D_2) = \int_{-\frac{h}{2}}^{\frac{h}{2}}\frac{E(z)}{2(1+v)}(1, z, z^2)dz \quad (10)$$

2.2. Reformulation of equilibrium equations

Upon substitution of Eqs. (3) and (4) into (9) and the subsequent results into the equilibrium equations in (5), five nonlinear coupled differential equations in terms of u, v, Ψ_r, Ψ_θ and w are obtained, which are complicated and difficult to be solved analytically. In order to facilitate their solution, the equilibrium equations are uncoupled to three equations. To this end, the boundary layer function Φ and the force function F are defined as follows [19, 20]:

$$\Phi(r,\theta)=\frac{1}{r}(\psi_{r,\theta}-(r\psi_\theta)_{,r})$$
$$N_r=\frac{1}{r}F_{,r}+\frac{1}{r^2}F_{,\theta\theta} \tag{11}$$
$$N_{r\theta}=-(\frac{1}{r}F_{,\theta})_{,r} \quad ,N_\theta=F_{,rr}$$

and using a procedure introduced in [20], the equilibrium equations in (5) are reformulated into three equations including one linear second-order equation in terms of the boundary layer function Φ and two nonlinear fourth-order equations in terms of transverse deflection, w and stress function, F as follows:

$$\nabla^2\Phi-\frac{K^2A_2}{\widehat{D}}\Phi=0 \tag{12}$$

$$\nabla^2\nabla^2 w=-\frac{1}{D}(P_z-N_1) \tag{13a}$$
$$+\frac{1}{K^2A_2}\nabla^2(P_z-N_1)-\frac{2\bar{C}}{A_1D}\frac{1}{r^2}N_2$$

$$\nabla^2\nabla^2 F=-\frac{2\bar{C}}{A_1D}(P_z-N_1) \tag{13b}$$
$$+\frac{\bar{A}A_1D-4\bar{C}^2}{A_1^2D}\frac{1}{r^2}N_2$$

where ∇^2 is the two-dimensional Laplace operator in polar coordinates and

$$D=D_1-\frac{B_1^2}{A_1} \quad ,\widehat{D}=D_2-\frac{B_2^2}{A_2}$$
$$\bar{A}=4A_2(A_1-A_2) \quad ,\bar{C}=A_1B_2-A_2B_1 \tag{14}$$

$$N_2=\tfrac{1}{r^2}\left(w_{,\theta}\right)^2+(w_{,r\theta})^2-rw_{,r}w_{,rr} \tag{15}$$
$$-\frac{2}{r}w_{,\theta}w_{,r\theta}-w_{,rr}w_{,\theta\theta}$$

Eqs. (12) and (13) are known, respectively, as the edge zone equation and interior equations of the plate. The other displacement field variables, i.e. u, v, Ψ_r, and Ψ_θ can be obtained from the following relations [20]:

$$\Psi_r=-w_{,r}-\frac{2\bar{C}}{\bar{A}K^2A_2}(\nabla^2F)_{,r}+\frac{\widehat{D}}{K^2A_2}\frac{1}{r}\Phi_{,\theta} \tag{16a}$$
$$-\frac{\bar{D}}{K^2A_2}[\nabla^2w-\frac{1}{K^2A_2}(P_Z-N_1)]_{,r}$$

$$\Psi_\theta=-\frac{1}{r}w_{,\theta}-\frac{2\bar{C}}{\bar{A}K^2A_2}\frac{1}{r}(\nabla^2F)_{,\theta} \tag{16b}$$
$$-\frac{\widehat{D}}{K^2A_2}\Phi_{,r}-\frac{\bar{D}}{K^2A_2}\frac{1}{r}$$
$$\times\left[\nabla^2w-\frac{1}{K^2A_2}(P_z-N_1)\right]_{,\theta}$$

$$u_{,r}=-\frac{1}{2}\left(w_{,r}\right)^2+\frac{A_1}{\bar{A}}\nabla^2F-\frac{1}{2A_2}F_{,rr} \tag{17a}$$
$$+\frac{B_2}{A_2}\frac{2\bar{C}}{\bar{A}K^2A_2}(\nabla^2F)_{,rr}-\frac{B_2}{A_2}\frac{\widehat{D}}{K^2A_2}L_2(\Phi)$$
$$+\frac{B_2}{A_2}w_{,rr}+\left(\frac{B_2}{A_2}\frac{\bar{D}}{K^2A_2}\frac{\partial^2}{\partial r^2}-\frac{2\bar{C}}{\bar{A}}\right)$$
$$\times\left[\nabla^2w-\frac{1}{K^2A_2}(P_z-N_1)\right]$$

$$\frac{1}{r}v_{,\theta}+\frac{u}{r}=-\frac{1}{2}\frac{1}{r^2}\left(w_{,\theta}\right)^2+\frac{A_1}{\bar{A}}\nabla^2F \tag{17b}$$
$$-\frac{1}{2A_2}L_1(F)+\frac{B_2}{A_2}\frac{2\bar{C}}{\bar{A}K^2A_2}L_1(\nabla^2F)$$
$$+\tfrac{B_2}{A_2}\tfrac{\widehat{D}}{K^2A_2}L_2(\Phi)+\tfrac{B_2}{A_2}L_1(w)$$
$$+(\frac{B_2}{A_2}\frac{\bar{D}}{K^2A_2}L_{1-}\frac{2\bar{C}}{\bar{A}})$$
$$\times\left[\nabla^2w-\frac{1}{K^2A_2}(P_z-N_1)\right]$$

$$\frac{1}{r}u_{,\theta}+v_{,r}-\frac{v}{r}=-\frac{1}{r}w_{,r}w_{,\theta}-\frac{1}{A_2}L_2(F) \tag{17c}$$
$$+\frac{B_2}{A_2}\frac{4\bar{C}}{\bar{A}K^2A_2}L_2(\nabla^2F)$$
$$+\frac{2B_2}{A_2}L_2(w)-\frac{B_2}{A_2}\frac{\widehat{D}}{K^2A_2}[L_2(\Phi)-\Phi_{,rr}]$$
$$+\frac{2B_2}{A_2}\frac{\bar{D}}{K^2A_2}L_2[\nabla^2w-\frac{1}{K^2A_2}(P_z-N_1)]$$

where $\bar{D}=(D_1\bar{A}-4A_2B_1^2+8A_2B_1B_2-4A_1B_2^2)/\bar{A}$ and the partial differential operators L_1 and L_2 are defined as:

$$L_1=\frac{1}{r}\frac{\partial}{\partial r}+\frac{1}{r^2}\frac{\partial^2}{\partial\theta^2}$$
$$L_2=\frac{\partial}{\partial r}(\frac{1}{r}\frac{\partial}{\partial\theta}) \tag{18}$$

2.3. Solution of the equations

Here, the non-linear differential Eqs. in (12), (13a), and (13b) are solved via the perturbation technique and Fourier series method. First, the three non-linear differential equations are replaced by an infinite set of linear differential equations using a perturbation technique. Then, the Fourier series expansions are utilized to reduce each set of

linear partial differential equations to ordinary ones, which are then analytically solved.

In order to solve the Eqs. (12), (13a), and (13b) using the perturbation technique, all unknown variables Φ, w, and F as well as the transverse loading P_z are expanded in ascending power series:

$$(\Phi, w, F)(r,\theta) = \sum_{k=1}^{\infty} ((\Phi_k, w_k, F_k)(r,\theta))\,\bar{w}_0^k \tag{19a}$$

$$P_z(r,\theta) = \sum_{k=1}^{\infty} P_{zk}(r,\theta)\,\bar{w}_0^k \tag{19b}$$

where the perturbation parameter $\bar{w}_0 = \mathrm{w}(r_1,\theta_1)/h$ is the non-dimensional maximum deflection of the sector plate. The definition of $\bar{w}_0$ requires that

$$\mathrm{w}_1(r_1,\theta_1) = \mathrm{h}\,,\ \mathrm{w}_k(r_1,\theta_1) = 0,\ k = 2,3,\ldots. \tag{20}$$

Substituting (19) into (12) and (13) and collecting the terms having the same order of $\bar{w}_0$ yields an infinite set of linear partial differential equations as follows:

$$\nabla^2\Phi_k - \frac{K^2A_2}{\widehat{D}}\Phi_k = 0 \tag{21}$$

$$\nabla^2\nabla^2 w_k = -\frac{1}{D}(P_{zk} - N_{1k}) + \frac{1}{K^2A_2}\nabla^2(P_{zk} - N_{1k}) - \frac{2\bar{C}}{A_1 D}\frac{1}{r^2}N_{2k} \tag{22}$$

$$\nabla^2\nabla^2 F_k = -\frac{2\bar{C}}{A_1 D}(P_{zk} - N_{1k}) + \frac{\bar{A}A_1 D - 4\bar{C}^2}{A_1^2 D}\frac{1}{r^2}N_{2k} \tag{23}$$

where N_{1k} and N_{2k}, which can be considered as pseudo loads at each perturbation step, are determined from the preceding perturbation step and are given as follows:

$$\begin{aligned}
&\bar{w}_0(k=1);\ N_{11}=0;\ N_{21}=0\\
&\bar{w}_0^k\ (k=2,3,\ldots);\\
&N_{1k} = \sum_{s=1}^{k-1}[\ell_1(F_s, w_{(k-s)}) + \ell_1(w_s, F_{(k-s)}) + \ell_2(F_s, w_{(k-s)})]\\
&N_{2k} = \sum_{s=0}^{k-s}[\ell_3(w_s, w_{(k-s)}) + \ell_4(w_s, w_{(k-s)})]
\end{aligned} \tag{24}$$

where the partial differential operators ℓ_1, ℓ_2, ℓ_3, and ℓ_4 are defined as:

$$\ell_1(,) = L_1()\frac{\partial^2()}{\partial r^2},\ \ell_2(,) = -2L_2()L_2() \tag{25}$$

$$\ell_3(,) = \left(\frac{1}{r}\frac{\partial}{\partial\theta} - \frac{\partial^2}{\partial r\partial\theta}\right)\left(\frac{1}{r}\frac{\partial}{\partial\theta} - \frac{\partial^2}{\partial r\partial\theta}\right)$$

$$\ell_4(,) = -\left(\frac{\partial^2}{\partial r^2}\right)\left(r\frac{\partial}{\partial r} + \frac{\partial^2}{\partial\theta^2}\right)$$

And in order to find Ψ_r, Ψ_θ, u and v, they are also expanded in ascending power series as follows:

$$(\Psi_r, \Psi_\theta, u, v)(r,\theta) = \sum_{k=1}^{\infty}((\Psi_{rk}, \Psi_{\theta k}, u_k, v_k)(r,\theta))\,\bar{w}_0^k \tag{26}$$

Substituting (26) and (19) into (16) and (17) and collecting the terms having the same order of $\bar{w}_0$ yields, respectively, an infinite set of linear relations as follows:

$$\begin{aligned}
\Psi_{rk} &= -w_{k,r} - \frac{2\bar{C}}{\bar{A}K^2A_2}(\nabla^2F_k)_{,r}\\
&- \frac{\bar{D}}{K^2A_2}[\nabla^2 w_k - \frac{1}{K^2A_2}(P_{zk} - N_{1k})]_{,r}\\
&+ \frac{\widehat{D}}{K^2A_2}\frac{1}{r}\Phi_{k,\theta}
\end{aligned} \tag{27a}$$

$$\begin{aligned}
\Psi_{\theta k} &= -\frac{1}{r}w_{k,\theta} - \frac{2\bar{C}}{\bar{A}K^2A_2}\frac{1}{r}(\nabla^2F_k)_{,\theta}\\
&- \frac{\bar{D}}{K^2A_2}\frac{1}{r}[\nabla^2 w_k - \frac{1}{K^2A_2}(P_{zk} - N_{1k}]_{,\theta}\\
&- \frac{\widehat{D}}{K^2A_2}\Phi_{k,r}
\end{aligned} \tag{27b}$$

$$\begin{aligned}
u_{k,r} &= NL_{1k} + \frac{A_1}{\bar{A}}\nabla^2F_k - \frac{1}{2A_2}F_{k,rr}\\
&+ \frac{B_2}{A_2}\frac{2\bar{C}}{\bar{A}K^2A_2}(\nabla^2F_k)_{,rr} - \frac{B_2}{A_2}\frac{\widehat{D}}{K^2A_2}L_2(\Phi_k)\\
&+ \frac{B_2}{A_2}w_{k,rr} + \left(\frac{B_2}{A_2}\frac{\bar{D}}{K^2A_2}\frac{\partial^2}{\partial r^2} - \frac{2\bar{C}}{\bar{A}}\right)\\
&\times[\nabla^2 w_k - \frac{1}{K^2A_2}(P_{zk} - N_{1k})
\end{aligned} \tag{28a}$$

$$\begin{aligned}
\frac{1}{r}v_{k,\theta} + \frac{u_k}{r} &= NL_{2k} + \frac{A_1}{\bar{A}}\nabla^2F_k - \frac{1}{2A_2}L_1(F_k)\\
&+ \frac{B_2}{A_2}\frac{2\bar{C}}{\bar{A}K^2A_2}L_1(\nabla^2F_k) + \frac{B_2}{A_2}\frac{\widehat{D}}{K^2A_2}L_2(\Phi_k)\\
&+ \frac{B_2}{A_2}L_1(w_k) + \left(\frac{B_2}{A_2}\frac{\bar{D}}{K^2A_2}L_1 - \frac{2\bar{C}}{\bar{A}}\right)\\
&\times\left[\nabla^2 w_k - \frac{1}{K^2A_2}(P_{zk} - N_{1k})\right]
\end{aligned} \tag{28b}$$

$$\begin{aligned}
\frac{1}{r}u_{k,\theta} + v_{k,r} - \frac{v_k}{r} &= NL_{3k} - \frac{1}{A_2}L_2(F_k)\\
&+ \frac{B_2}{A_2}\frac{4\bar{C}}{\bar{A}K^2A_2}L_2(\nabla^2F_k) + \frac{2B_2}{A_2}L_2(w_k)\\
&- \frac{B_2}{A_2}\frac{\widehat{D}}{K^2A_2}[L_1(\Phi_k) - \Phi_{k,rr}]\\
&+ \frac{2B_2}{A_2}\frac{\bar{D}}{K^2A_2}L_2[\nabla^2 w_k - \frac{1}{K^2A_2}(P_{zk} - N_{1k})]
\end{aligned} \tag{28c}$$

where

$$\bar{w}_0; NL_{11}=0; NL_{21}=0; NL_{31}=0$$
$$\bar{w}_0^k;\ NL_{1k}=-\frac{1}{2}\sum_{s=1}^{k-s} w_{s,r}w_{(k-s),r}\ ;$$
$$NL_{2k}=-\frac{1}{2}\frac{1}{r^2}\sum_{s=1}^{k-s} w_{s,\theta}w_{(k-s),\theta}\ ; \tag{29}$$
$$NL_{3k}=-\frac{1}{r}\sum_{s=1}^{k-s} w_{s,r}w_{(k-s),\theta}$$

Next, in order to solve the linear partial differential equations within each set of perturbation step, Fourier series method is employed. To this end, it is assumed that the radial edges at $\theta = 0$ and $\theta = \theta_0$ have simple supports with following boundary conditions:

$$M_{\theta k}=\Psi_{rk}=w_k=0, u_k=N_{\theta k}=0 \tag{30}$$

In order to satisfy the boundary conditions at radial edges (30), the unknown variables and pressure are represented as a single Fourier series as follows:

$$(\tilde{F}_k,\tilde{w}_k,\tilde{\Psi}_{rk},\tilde{u}_k)(r,\theta)=\sum_{m=1}^{\infty}(\tilde{F}_{km}(r),\tilde{w}_{km}(r),\tilde{\Psi}_{rkm}(r),\tilde{u}_{km}(r))\sin(\alpha_m\theta)$$
$$(\Phi_{km},\Psi_{\theta k},v_k)(r,\theta)=\sum_{m=0}^{\infty}(\Phi_{km}(r),\Psi_{\theta km}(r),v_{km}(r))\cos(\alpha_m\theta)$$
$$P_{zk}(r,\theta)=\sum_{m=1}^{\infty}\tilde{P}_{km}(r)\sin(\alpha_m\theta) \tag{31}$$

where $\alpha_m = m\pi/\theta_0$. Substitution of Eq. (31) into Eq.(21) through (23) and Eqs. (27) and (28), yields ordinary differential equations whose general solutions are known to be as follows:

$$\Phi_{km}(r)=A_{1km}I_{\alpha_m}(\mu r) \tag{32}$$

$$\tilde{w}_{km}=-\frac{1}{D}\{\tilde{q}_{1km}-\tilde{\mathcal{X}}_{1km}\}+\frac{1}{K^2A_2}\{\tilde{q}_{2km}-\tilde{\mathcal{X}}_{2km}\}-\frac{2\bar{C}}{A_1D}\bar{\Omega}_{1km}+\tilde{D}_{1km}r^{\alpha_m}+\tilde{D}_{2km}r^{\alpha_m+2} \tag{33}$$

$$\tilde{F}_{km}=-\frac{2\bar{C}}{A_1D}\{\tilde{q}_{1km}-\tilde{\mathcal{X}}_{1km}\}+\frac{\bar{A}A_1D-4\bar{C}^2}{A_1^2D}\tilde{\Omega}_{1km}+\tilde{B}_{1km}r^{\alpha_m}+\tilde{B}_{2km}r^{\alpha_m+2} \tag{34}$$

$$\tilde{\Psi}_{rkm}=\frac{1}{D}\left(\tilde{q}'_{1km}-\tilde{\mathcal{X}}'_{1km}\right)+\hat{C}(\tilde{q}'_{2km}-\tilde{\mathcal{X}}'_{2km})+\frac{2\bar{C}\hat{C}}{A_1}\tilde{\Omega}'_{2km}+\frac{2\bar{C}}{A_1D}\tilde{\Omega}'_{1km}-\frac{\alpha_m}{r\mu^2}(A_{1km}I_{\alpha m}(\mu r))$$
$$-\alpha_m r^{\alpha_m-1}\begin{Bmatrix}\tilde{D}_{1km}+\dfrac{8\bar{C}(\alpha_m+1)}{\bar{A}K^2A_2}\tilde{B}_{2km}+\\ \dfrac{4\bar{D}(\alpha_m+1)}{K^2A_2}\tilde{D}_{2km}\end{Bmatrix}-(\alpha_m+2)r^{\alpha_m+1}(\tilde{D}_{2km}) \tag{35}$$

$$\Psi_{\theta km}=\frac{\alpha_m}{r}\frac{1}{D}\{\tilde{q}_{1km}-\tilde{\mathcal{X}}_{1km}\}+\frac{2\bar{C}}{A_1D}\frac{\alpha_m}{r}\tilde{\Omega}_{1km}+\frac{\hat{C}\alpha_m}{r}\{\tilde{q}_{2km}-\tilde{\mathcal{X}}_{2km}\}+\frac{2\bar{C}\hat{C}}{A_1}\frac{\alpha_m}{r}\tilde{\Omega}_{2km}-\frac{\widehat{D}}{K^2A_2}\{A_{1km}\frac{d}{dr}\{I_{\alpha m}(\mu r)\}-\alpha_m r^{\alpha_m+1}\tilde{D}_{2km}$$
$$-\alpha_m r^{\alpha_m-1}\begin{Bmatrix}\tilde{D}_{1km}+\frac{8\bar{C}}{\bar{A}K^2A_2}(\alpha_m+1)\tilde{B}_{2km}\\ +\frac{4(1+\alpha_m)}{K^2A_2}\bar{D}\tilde{D}_{2km}\end{Bmatrix} \tag{36}$$

$$\tilde{u}_{km}=\left(\frac{\bar{C}}{A_1}-B_2\right)\frac{1}{A_2D}\{\tilde{q}'_{1km}-\tilde{\mathcal{X}}'_{1km}\}-\tilde{C}\tilde{\Omega}'_{1km}-\frac{B_2}{A_2}\hat{C}\{\tilde{q}'_{2km}-\tilde{\mathcal{X}}'_{2km}\}-\frac{B_2}{A_2}\frac{2\bar{C}\hat{C}}{A_1}\tilde{\Omega}'_{2km}+\int\tilde{\Omega}_{2km}dr+\frac{B_2}{A_2}\frac{\widehat{D}}{K^2A_2}\frac{\alpha_m}{r}\{A_{1km}I_{\alpha_m}(\mu r)\}+\int\widetilde{NL}_{1km}dr$$
$$+\alpha_m r^{\alpha_m-1}\begin{Bmatrix}-\dfrac{\tilde{B}_{1km}}{2A_2}+\\ \dfrac{B_2}{A_2}\left(\begin{matrix}\dfrac{8\bar{C}(\alpha_m+1)}{\bar{A}K^2A_2}\tilde{B}_{2km}\\ +\tilde{D}_{1km}+\dfrac{4\bar{D}(\alpha_m+1)}{K^2A_2}\tilde{D}_{2km}\end{matrix}\right)\end{Bmatrix}+r^{\alpha_m+1}\begin{Bmatrix}\left(\dfrac{4A_1}{\bar{A}}-\dfrac{(\alpha_m+2)}{2A_2}\right)\tilde{B}_{2km}\\ +\left(\dfrac{B_2(\alpha_m+2)}{A_2}-\dfrac{8\bar{C}}{\bar{A}}\right)\tilde{D}_{2km}\end{Bmatrix} \tag{37}$$

$$v_{km}=-\frac{r}{\alpha_m}\widetilde{NL}_{2km}+\frac{1}{\alpha_m}\int\widetilde{NL}_{1km}dr-\frac{\tilde{C}\alpha_m}{r}\tilde{\Omega}_{1km}+(\frac{\bar{C}}{A_1}-B_2)\frac{\alpha_m}{rDA_2}\times\{\tilde{q}_{1km}-\tilde{\chi}_{1km}\}-\frac{r}{\alpha_m}\tilde{\Omega}_{2km}+\frac{B_2}{A_2}\frac{\widehat{D}}{K^2A_2}\frac{d}{dr}\{A_{1km}I_{\alpha_m}(\mu r)\}+\frac{1}{\alpha_m}\int\tilde{\Omega}_{2km}dr$$
$$+r^{\alpha_m+1}\begin{Bmatrix}-\left(\dfrac{4A_1}{\bar{A}}+\dfrac{\alpha_m}{2A_2}\right)\tilde{B}_{2km}\\ +\left(\dfrac{8\bar{C}}{\bar{A}}+\dfrac{B_2}{A_2}\alpha_m\right)\tilde{D}_{2km}\end{Bmatrix}+r^{\alpha_m-1}\alpha_m\times\left\{-\frac{\tilde{B}_{1km}}{2A_2}+\frac{B_2}{A_2}\begin{Bmatrix}\dfrac{8\bar{C}}{\bar{A}K^2A_2}(\alpha_m+1)\tilde{B}_{2km}+\tilde{D}_{1km}\\ +\dfrac{4\bar{D}}{K^2A_2}(\alpha_m+1)\tilde{D}_{2km}\end{Bmatrix}\right\}$$
$$-\hat{C}\frac{B_2}{A_2}\frac{\alpha_m}{r}\{\tilde{q}_{2km}-\tilde{\chi}_{2km}\}-\frac{B_2}{A_2}\frac{2\bar{C}\hat{C}}{A_1}\frac{\alpha_m}{r}\tilde{\Omega}_{2km} \tag{38}$$

where I_{α_m} is the modified Bessel function of the first kind and:

$$\hat{C} = \frac{1}{K^2 A_2}\left[\frac{4\bar{C}^2}{\bar{A}A_1 D} - \left(1 - \frac{\bar{D}}{D}\right)\right]$$
$$\tilde{C} = \frac{1}{A_2 A_1 D}\left(\frac{\bar{A}A_1 D - 4\bar{C}^2}{2A_1} + 2B_2\bar{C}\right) \quad (39)$$
$$\mu = \sqrt{\frac{K^2 A_2}{\bar{D}}}$$

Also

$$\{\tilde{q}_{1km}, \tilde{\chi}_{1km}, \tilde{\Omega}_{1km}\} = \frac{1}{r^{\alpha_m}} \int \frac{1}{r^{1-2\alpha_m}} \int \frac{1}{r^{2\alpha_m - 1}}$$
$$\times \int \frac{1}{r^{1-2\alpha_m}} \int \frac{1}{r^{\alpha_m - 1}} \left\{\tilde{P}_{km}, \tilde{N}_{1km}, \frac{\tilde{N}_{2km}}{r^2}\right\} drdrdrd$$
$$\{\tilde{q}_{2km}, \tilde{\chi}_{2km}, \tilde{\Omega}_{2km}\} = \frac{1}{r^{\alpha_m}} \int \frac{1}{r^{1-2\alpha_m}} \quad (40)$$
$$\int \frac{1}{r^{\alpha_m - 1}} \left\{\tilde{P}_{km}, \tilde{N}_{1km}, \frac{\tilde{N}_{2km}}{r^2}\right\} drdr$$

It is to be noted that in Eqs. (32)-(38) A_{1km}, $\tilde{B}_{1km}$, $\tilde{B}_{2km}$, $\tilde{D}_{1km}$ and $\tilde{D}_{2km}$ are the integration constants in each perturbation step. These unknown constants are determined by imposing the appropriate boundary conditions at $r = b$. Here, clamped and simply supported boundary conditions are considered at the circular edge ($r = b$) as follows:

$$\text{C}: \Psi_{rk} = \Psi_{\theta k} = w_k = 0, u_k = v_k = 0 \quad (41)$$

$$\text{S}: M_{rk} = \Psi_{\theta k} = w_k = 0, u_k = v_k = 0 \quad (42)$$

In each perturbation step, by imposing boundary conditions at $r = b$, the integration constants are obtained in terms of the unknown constants $\tilde{P}_{km}$. On the other hand, these unknown parameters are determined upon substitution of (33) into (20). Finally, the perturbation parameter $\bar{w}_0$ is found from Eq. (19b) which is a non-linear polynomial equation in $\bar{w}_0$ and is solved here numerically.

3. Numerical results and discussions

Here, to validate the results of the present study, three validation examples are presented for linear and nonlinear bending problems of circular sector plates with simply supported radial edges. For the purpose of numerical illustrations, Aluminum–Zirconia as a system of FG is considered. The material properties of Aluminum and Zirconia are, respectively, assumed to be $E_m = 70\,GPa$, $\upsilon_m = 0.3$, and $E_c = 151\,GPa$, $\upsilon_c = 0.3$ [9, 21]. In all calculations, the shear correction factor is taken to be 5/6.

Example 1. The numerical results for the linear bending of FG circular sector plate with clamped and simple supports at the circular edge, subjected to a uniform transverse pressure ($P_z(r,\theta) = p_0$) are pesented in Fig. 2 and are compared with those presented by Fallah and Nosier in [9]. Variations of non-dimensional transverse deflection ($w^* = wE_c h^2/p_0 b^3$) in radial direction ($\theta = \pi/18$) for an FG sector plate with $h/b = 0.1$, $\theta_0 = \pi/3$ and $n = 3$ are shown in Fig. 2. It is worth mentioning that the results obtained in the first perturbation step represent a linear bending analysis. It is seen in Fig. 2 that the first-perturbation solution is in excellent agreement with the analytical solution presented in [9].

Example 2. The numerical results for linear bending of homogeneous circular sector plates with various vertex angles subjected to a uniform transverse pressure, p_0, are obtained within the classical plate theory ($K^2 A_2 \to \infty$) and compared with those presented by Timoshenko and Woinowsky [22]. The results for non-dimensional deflection $\overline{w} = w\tilde{D}/p_0 b^4$ (with $\tilde{D} = Eh^3/12(1-\nu^2)$) at some points on the symmetry axis of the sector ($\theta = \theta_0/2$) are presented in Table 1 and Table 2 for, respectively, clamped and simple supports at the circular edge. Excellent agreements are seen to exist between the two results.

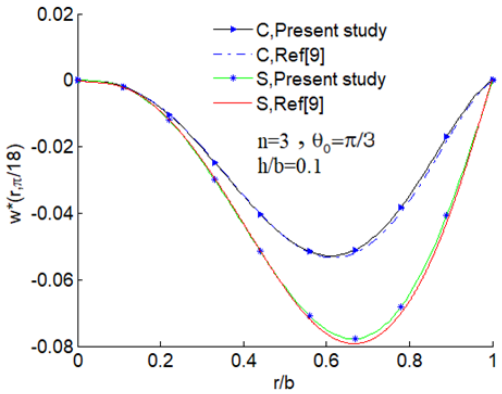

Fig. 2. Comparison of linear non-dimensional transverse deflection of FG circular sector plate with clamped and simple supports at the circular edge

Table 1. Comparison of linear non-dimensional transverse deflection of a homogenous circular sector plate with clamped support at the circular edge under a uniform pressure

θ_0	$\bar{w}$	Ref. [22]	Present study
$\pi/3$	$\bar{w}(0.25b,\theta_0/2)$	0.00017	0.000159
	$\bar{w}(0.5b,\theta_0/2)$	0.00057	0.000568
	$\bar{w}(0.75b,\theta_0/2)$	0.00047	0.000479
$\pi/2$	$\bar{w}(0.25b,\theta_0/2)$	0.00063	0.000634
	$\bar{w}(0.5b,\theta_0/2)$	0.00132	0.001300
	$\bar{w}(0.75b,\theta_0/2)$	0.00082	0.000849

Table 2. Comparison of linear non-dimensional transverse deflection of a homogenous circular sector plate with simple support at the circular edge under a uniform pressure

θ_0	$\bar{w}$	Ref. [22]	Present study
$\pi/3$	$\bar{w}(0.25b,\theta_0/2)$	0.00019	0.000196
	$\bar{w}(0.5b,\theta_0/2)$	0.00080	0.000802
	$\bar{w}(0.75b,\theta_0/2)$	0.00092	0.000939
$\pi/2$	$\bar{w}(0.25b,\theta_0/2)$	0.00092	0.000926
	$\bar{w}(0.5b,\theta_0/2)$	0.00225	0.002300
	$\bar{w}(0.75b,\theta_0/2)$	0.00203	0.002100

Example 3. The numerical results for nonlinear bending analysis of homogenous isotropic sector plates with simple supports at circular edges, subjected to a uniform transverse pressure ($P_z(r,\theta)=p_0$) are presentd in Fig. 3 and are compared with those presented by Turvey and Salehi in [14]. Variations of non-dimensional maximum deflection $w^*=w/h$ versus dimensionless load $p^*=p_0b^4/E_mh^4$ for a homogenous isotropic sector plate with $h/b=0.2$ and $\theta_0=\pi/3$ are depicted in Fig. 3. The maximum deflection occurs at $r=0.647\,b$ and $\theta=\theta_0/2=\pi/6$. The results obtained within this study are in good agreement with those in [14].

In the remainder of the present work, linear and nonlinear bending of FG circular sector plates under a uniform transverse pressure ($P_z(r,\theta)=p_0$) is considered. Unless mentioned otherwise, the thickness to radius ratio h/b and vertex angle θ_0 of the plate are assumed to be 0.02 and $\pi/3$, respectively, and the results will be presented for $\theta=\theta_0/2$ and $n=1$. For convenience, the following non-dimensional parameters are introduced:

$$w^*=w/h$$
$$p^*=p_0b^4/E_mh^4 \qquad (43)$$
$$N_r^*=N_rb^2/E_ch^3$$

Figs. 4 and 5 show a comparison of linear (first-step perturbation solution) and nonlinear analyses for the variations of non-dimensional maximum deflection versus pressure in FG sector plates with simple and clamped supports at circular edge, respectively. It is observed that the difference between linear and nonlinear analyses (a discrepancy more than 2 percent) starts from $w/h=0.25$ for simple support and from $w/h=0.23$ for clamped support, which indicates the importance of nonlinear analysis for FG sectors.

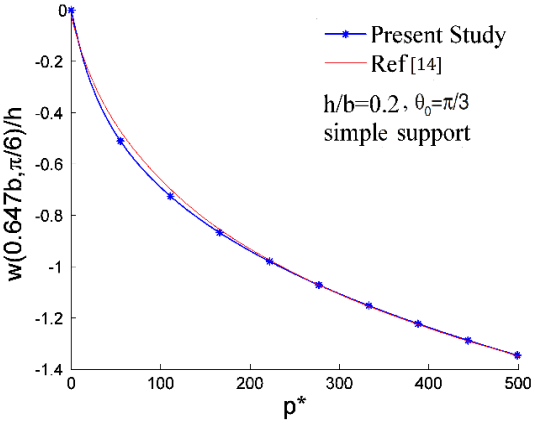

Fig. 3. Comparison of nonlinear bending results for a homogenous isotropic sector plate with simple supports at the circular edge.

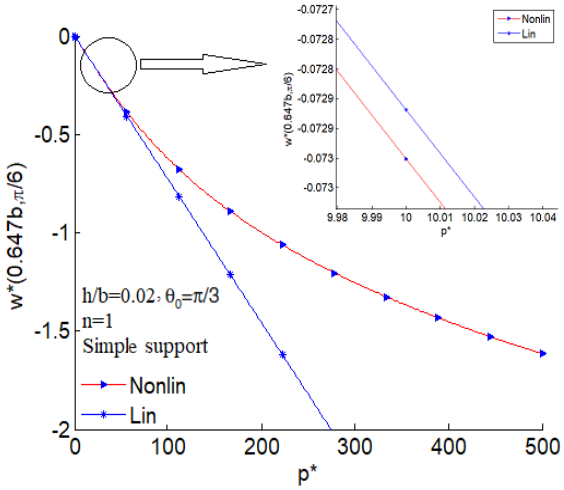

Fig. 4. Variations of maximum non-dimensional deflection of FG circular sector plates with simple supports at circular edge versus load parameter p^*.

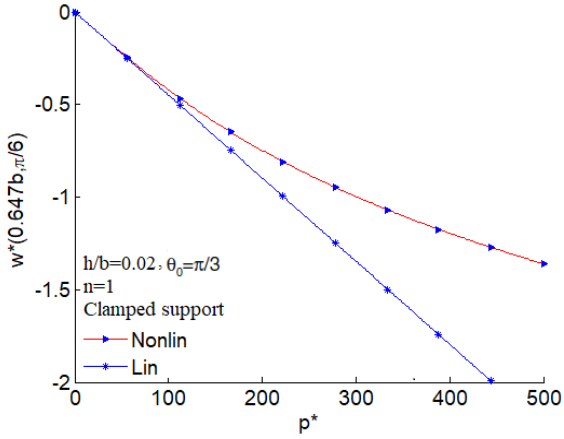

Fig. 5. Variations of maximum non-dimensional deflection of FG circular sector plates with clamped supports at circular edge versus load parameter p^*

Another phenomenon is observed in a fully simply supported FG sector plate (Fig. 4) where in a small region ($w/h \leq 0.1$), nonlinear analysis predicts the transvers deflection larger than the one linear analysis predicts which again emphasizes the importance of nonlinear analysis for FG material.

To explain such a behavior, a comparison of linear and non-linear analyses for the variations of non-dimensional radial resultant force versus pressure in FG sector plates with clamped and simple supports at their circular edge, are investigated in Figs. 6 and 7, respectively. It is seen in Fig. 6 that the radial resultant force of clamped sector plate is always positive according to the non-linear theory. However, according to the non-linear solution in Fig. 7, it is observed that the radial resultant force N_r is always tensile except in a small region in the beginning of a positive transverse load in which N_r is compressive due to the existing bending–extension coupling in the plate and then becomes tensile as the loading is increased (since the large deformation effect becomes dominant). This can explain the behavior in a fully simply supported FG sector plate that the nonlinear deflection is larger than the linear one, since compressive radial force has a softening effect. Further numerical results show that this phenomenon is more pronounced in FG plates with stronger bending-extension coupling. This observation is also reported in [23].

The results for dimensionless deflection of simply supported and clamped FG sector plate under uniform pressure ($p^* = 200$) for different values of power-law index, n, along the radial direction at $\theta = \theta_0/2$ are shown in Fig. 8. The maximum deflection happens at $r = 0.601\,b$ for clamped supports and at $r = 0.651\,b$ for simple supports. It is expectedly observed that for higher values of n, where the volume fraction of metal increases, the plate deflection increases, too. Furthermore, the deflection of an FG sector plate with simple supports at the circular edge is larger than the one with clamped supports.

4. Conclusions

In the present work, the von Karman nonlinear equilibrium equations of an FG sector plate subjected to transverse mechanical load within FSDT are reformulated. An analytical solution is developed for FG circular sector plates with simple supports at the radial edges using perturbation technique in conjunction with Fourier series method. The results are verified with the known results in the literature. Effects of material constant and nonlinearity on FG sector plates with various boundary conditions is studied in several numerical illustrations. Comparison of the linear and nonlinear analyses shows that linear analysis is only valid for $w/h < 0.2$ and is inadequate for analysis of fully simply supported FG sector plates even in the small deflection range, which, on the other hand, shows the importance of a nonlinear analysis. Furthermore, the results presented here based on the analytical solution can be used as a benchmark in future studies.

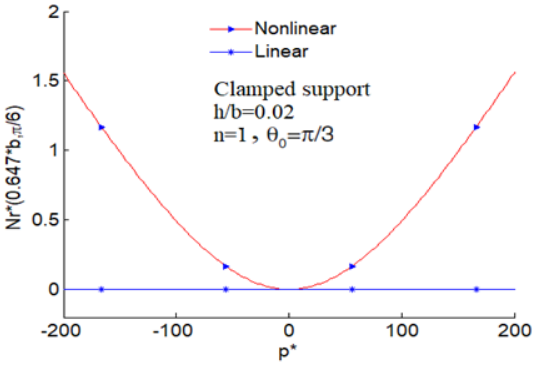

Fig. 6. Variations of non-dimensional radial stress resultant of FG circular sector plates with clamped supports at circular edge versus load parameter p^*

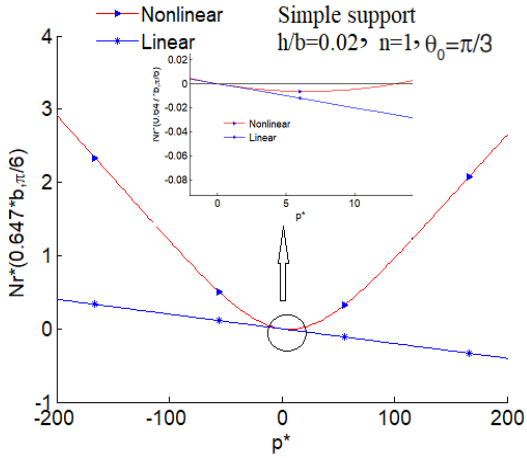

Fig. 7. Variations of non-dimensional radial stress resultant of FG circular sector plates with simple supports at circular edge versus load parameter p^*

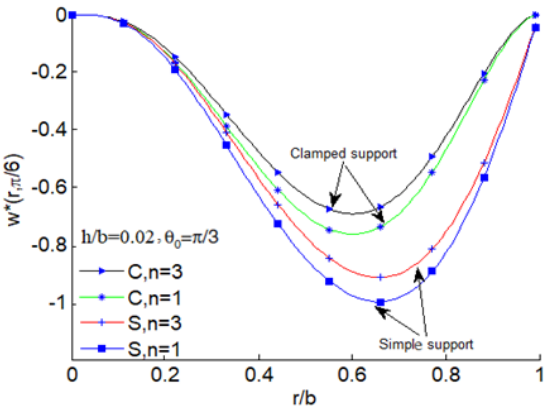

Fig. 8. Dimensionless deflection of FG sector plates under uniform pressure ($p^* = 200$) for different values of n along the radial direction at $\theta = \theta_0/2$

References

[1] Koizumi MFGM. FGM activities in Japan. *Composites Part B: Engineering* 1997; 28(1-2): 1-4.

[2] Jha DK, Kant T, Singh RK. A critical review of recent research on functionally graded plates. *Composite Structures* 2013; 96: 833-849.

[3] Kobayashi H, Turvey GJ. Elastic small deflection analysis of annular sector Mindlin plates. *International journal of mechanical sciences* 1994; 36(9); 811-827.

[4] Ambartsumian SA. **Theory of anisotropic plates: strength, stability, vibration**. Technomic Publishing Company; 1970.

[5] Cheung MS, Chan MYT. Static and dynamic analysis of thin and thick sectorial plates by the finite strip method. *Computers & Structures* 1981; 14(1-2): 79-88.

[6] Liu FL, Liew KM. Differential quadrature element method for static analysis of Reissner–Mindlin polar plates. *International Journal of Solids and Structures* 1999; 36(33): 5101-5123.

[7] Lim GT, Wang CM. Bending of annular sectorial Mindlin plates using Kirchhoff results. *European Journal of Mechanics-A/Solids* 2000; 19(6): 1041-1057.

[8] Jomehzadeh E, Saidi AR, Atashipour SR. An analytical approach for stress analysis of functionally graded annular sector plates. *Materials & design* 2009; 30(9): 3679-3685.

[9] Fallah F, Nosier A. Thermo-mechanical behavior of functionally graded circular sector plates. *Acta Mechanica* 2015; 226(1): 37-54.

[10] Mousavi SM, Tahani M. Analytical solution for bending of moderately thick radially functionally graded sector plates with general boundary conditions using multi-term extended Kantorovich method. *Composites Part B: Engineering* 2012; 43(3): 1405-1416.

[11] Fereidoon A, Mohyeddin A, Sheikhi M, Rahmani H. Bending analysis of functionally graded annular sector plates by extended Kantorovich method. *Composites Part B: Engineering* 2012; 43(5): 2172-2179.

[12] Aghdam MM, Shahmansouri N, Mohammadi M. Extended Kantorovich method for static analysis of moderately thick functionally graded sector plates. *Mathematics and Computers in Simulation* 2012; 86: 118-130.

[13] Fallah F, Khakbaz A. On an extended Kantorovich method for the mechanical behavior of functionally graded solid/annular sector plates with various boundary conditions. *Acta Mechanica* 2017; 228(7): 2655-2674.

[14] Turvey GJ, Salehi M. DR large deflection analysis of sector plates. *Computers & Structures* 1990; 34(1): 101-112.

[15] Alinaghizadeh F, Kadkhodayan M. Large deflection analysis of moderately thick radially functionally graded annular sector plates fully and partially rested on two-parameter elastic foundations by GDQ method. *Aerospace Science and Technology* 2014; 39: 260-271.

[16] Golmakani ME, Kadkhodayan M. Large deflection thermoelastic analysis of functionally graded stiffened annular sector plates. *International Journal of Mechanical Sciences* 2013; 69: 94-106.

[17] Fung YC, Tong P, Chen X. Classical and computational solid mechanics (Vol. 2). World Scientific Publishing Company; 2017.

[18] Reddy JN. **Theory and analysis of elastic plates and shells**. CRC press; 2006.

[19] Nosier A, Fallah F. Reformulation of Mindlin–Reissner governing equations of functionally graded circular plates. *Acta Mechanica* 2008; 198(3-4): 209-233.

[20] Nosier A, Fallah F. Non-linear analysis of functionally graded circular plates under asymmetric transverse loading. *International journal of non-Linear mechanics* 2009; 44(8): 928-942.

[21] Najafizadeh MM, Eslami MR. First-order-theory-based thermoelastic stability of functionally graded material circular plates. *AIAA journal* 2002; 40(7): 1444-1450.

[22] Timoshenko SP, Woinowsky-Krieger S. **Theory of plates and shells**. McGraw-hill; 1959.

[23] Fallah F, Nosier A. Nonlinear thermo-mechanical cylindrical bending of functionally graded plates. *Proc. IMechE, Part C: J. Mech. Eng. Sci.* 2008; 222(C3): 305-318.